2019

The effect of a small vegetation dieback event on salt marsh sediment transport

Daniel J. Coleman
Virginia Institute of Marine Science

Matthew L. Kirwan
Virginia Institute of Marine Science

The effect of a small vegetation dieback event on salt marsh sediment transport

Daniel J. Coleman and Matthew L. Kirwan

Abstract

Vegetation is a critical component of the ecogeomorphic feedbacks that allow a salt marsh to build soil and accrete vertically. Vegetation dieback can therefore have detrimental effects on marsh stability, especially under conditions of rising sea levels. Here, we report a variety of sediment transport measurements associated with an unexpected, natural dieback in a rapidly prograding marsh in the Altamaha River Estuary, GA. We find that vegetation mortality led to a significant loss in elevation at the dieback site as evidenced by measurements of vertical accretion, erosion, and surface topography compared to vegetated reference areas. Belowground vegetation mortality led to reduced soil shear strength. The dieback site displayed an erosional, concave-up topographic profile, in contrast to the reference sites. At the location directly impacted by the dieback, there was a reduction in flood dominance of suspended sediment concentration. Our work illustrates how a vegetation disturbance can at least temporarily reverse the local trajectory of a prograding marsh and produce complex patterns of sediment transport.

Introduction

Ecogeomorphology—the study of geomorphic processes, ecological factors, and their interactions—is required to understand the evolution of numerous systems (Murray et al. 2008; Reinhardt et al. 2010). Such interactions dominate the topographic evolution of hill slopes (Saco et al. 2007, Pawlik et al. 2007), river floodplains (Steiger et al. 2005), beach dunes (Duran and Moore 2013), and salt marshes (Fagherazzi et al. 2004). Salt marshes are one of the classical ecogeomorphic systems, where two-way interactions shape the landscape and play a primary role in marsh stability (Redfield 1972, Reed 1995, Kirwan and Megonigal 2013, D'Alpaos and Marani, 2016). For example, elevation in the tidal frame is a major control on type and abundance of vegetation, which in turn promotes sediment deposition and thus affects elevation (Morris et al. 2002, Temmerman et al. 2003, Kirwan et al. 2010, Fagherazzi et al. 2012 and references therein). Animal activity also impacts marsh geomorphology; for example, grazing pressure from crabs can reduce vegetation and lead to sediment erosion (Hughes et al. 2009, Smith 2009, Smith and Green 2015).

Vegetation disturbances, or diebacks, are common in salt marshes, occurring throughout the world and affecting all elevations and geomorphic settings (Alber et al. 2008). Prominent examples include marshes from the Gulf Coast (DeLaune et al. 1994, Lindstedt et al. 2006, Day et al. 2011), southeastern (Silliman et al. 2005, Ogburn and Alber 2006, Alber et al. 2008, Li and Pennings 2016), and northeastern (Bertness and Ellison 1987, Holdredge et al. 2009, Smith 2009, Alteiri et al. 2013) regions of the U.S Atlantic Coast. For instance, in Louisiana in 2001, a statewide dieback reached 126,000 acres of marsh (Lindstedt et al. 2006). In Georgia, dieback affected 2,000 acres of

marsh in 2001-2002 (Ogburn and Alber 2006), and the region continues to experience smaller scale events (Alber et al. 2008). *Spartina alterniflora* is the most common species to die back, but a host of other salt marsh plants can as well (Alber et al. 2008). Similarly, all geomorphic features of the marsh such as the creek edge and interior exhibit such events (Alber et al. 2008).

The variety of sites impacted likely stems from the variety of causes of dieback. Vegetation dieback is often linked in part to drought (Silliman et al., 2005; Alber et al., 2008), but can also be caused by herbivory (Smith and Green, 2015; Silliman et al. 2005; Holdredge et al. 2009), salt stress (Hughes et al. 2012), soil toxicity (Mckee et al. 2004), oil spills (Silliman et al. 2012, Lin et al. 2016), wrack deposits (Fischer et al. 2000), and other factors. In some cases, a marsh can recover from a dieback (Ogburn and Alber 2006, Angelini and Silliman 2012, Alteiri et al. 2013). The 2001 Louisiana dieback shrank to approximately 13% its original size after two years, indicating significant recovery (Lindstedt et al. 2006). However, diebacks can also be permanent, especially if the marsh experiences erosion (Lottig and Fox 2007, Silliman et al. 2012), such that the marsh elevation becomes too low for vegetation to grow (Wang and Temmerman 2013; van Belzen et al. 2016).

Vegetation loss often causes erosion, through the combination of enhanced flow velocities and weaker soils (Temmerman et al. 2012, Lin et al. 2016). For example, oil-induced vegetation mortality that extended to the belowground parts of the plant resulted in increased edge erosion (Silliman et al. 2012). This erosion however, may act as a source of sediment for the surrounding marsh, enhancing overall resiliency to sea level rise (Mariotti and Carr 2014, Hopkinson et al. 2018). For example, the rapidly

eroding marsh complex of the Blackwater River (Maryland) had higher suspended sediment concentrations (SSC) and vertical accretion rates than a more stable adjacent system (Ganju et al. 2015).

Here, we study sediment transport before and after a small dieback event at a previously prograding marsh. We find that vegetation loss led to significant erosion and a local reversal of rapid marsh progradation.

Methods

Study Site and Approach

This study was conducted in a *Spartina alterniflora* marsh within the Altamaha River estuary system in Georgia, USA (31°17’59”N 81°24’24”W) (Figure 1). The lower Altamaha has a 2m tidal range and is characterized by expansive brackish and saline marshes (GCE LTER, https://gce-lter.marsci.uga.edu). Average salinities range from 5-20 PSU and average plant biomass ranges from approximately 1700-1000 g/m^2, respectively (Wieski et al. 2010). Our study site is a rapidly accreting, youthful salt marsh (<30 years old based off of aerial photography) located along a small tidal channel west of Little Broughton Island (Figure 1). The site ranges from approximately -0.8 m to +0.3 m mean sea level, based off the nearby vertical benchmark on St. Simon’s Island. Proximate dredging in the early 1970s led to channel network reorganization (Hardisky 1978), and progradation of marsh into an infilling channel at our site. Analysis of 8 historical photographs (earthexplorer.usgs.gov) indicates significant marsh progradation, reducing open water area from over 650,000 m^2 to less than 125,000 m^2 between 1975 and 2013 (Figure 2). As a result, the site is

characterized by a smooth topographic profile from channel to marsh platform without a scarp or levee, typical of concave-down, prograding marshes (Mariotti and Fagherazzi 2010).

The initial goal of this study was to monitor how seasonal vegetation growth influenced sediment transport across the marsh. We monitored sediment deposition rates, turbidity, and biomass along a transect from the channel to the marsh interior for an entire year. However, two months into the study, in early August 2016, vegetation began to die in a narrow band adjacent and parallel to the channel edge. By December 2016, the dieback reached its maximum spatial extent—over 6m in shore length and over 2m in width—and demonstrated erosive features such as exposed roots, gullies, and undercut equipment (Figure 3). The size of the dieback remained relatively constant through spring 2017 until there was some indication of recovery in early summer 2017. This unexpected event prevented us from evaluating the role of seasonal vegetation growth on suspended sediment dynamics, but allowed us to address how a dieback event influences marsh sediment transport and surface elevation. To address the impact of the dieback, we supplemented our seasonal monitoring with one time measures of soil shear strength, rhizome mortality, and elevation profiles.

Seasonal monitoring of sediment transport

We measured turbidity and sediment deposition along a transect from channel to marsh interior for 1 year, beginning in June 2016. We measured turbidity (NTU) with optical back scatter sensors to quantify sediment transport from the channel across the marsh. The transect consisted of three turbidity sensors in a shore normal transect, with

one in the channel (YSI 6600), and two on the marsh surface (referred to as the channel sensor and marsh sensors, respectively). The “marsh edge sensor” was 2.4m from the channel edge (Seapoint, RBR Solo) and the “marsh interior sensor” was 18m from the edge (Seapoint, RBR Duo; Figure 1c). The sensors measured every 15 minutes and were equipped with automatic wipers to reduce biofouling. Sensors were cleaned and maintained and the data downloaded on approximately bimonthly site visits. Following retrieval, the turbidity time series data was filtered to remove any erroneous points and times when the sensors were fouled or exposed (Ganju et al. 2005).

Turbidity data was converted to suspended sediment concentration (SSC) via a combination of in situ field sampling and laboratory calibrations using sediment collected from the site. In the field, we measured turbidity with an additional sensor at various locations around the site and at different tidal stages, and collected a water sample in conjunction with each reading. In the lab, we created sediment-water slurries with a range of SSC and used a turbidity sensor to measure the slurries while they were kept in constant motion to avoid sediment settling. We compared sensor turbidity measurements to total suspended solid measurements obtained via vacuum filtration of water samples from the site and lab-created water-sediment slurries. The y-intercept value was set to zero, resulting in the equation SSC (mg/L) =1.33*Sensor Turbidity (NTU) (R^2=0.9345, n=26, p<<0.001). The data was then divided into pre-dieback (June 1, 2016-August 31, 2016) and post-dieback (September 1, 2016-April 18, 2017) periods. We calculated the average SSC for each sensor when all sensors were flooded for both time periods. The channel sensor also recorded water pressure which we converted to water depth by adjusting for barometric pressure. We then separated the turbidity time

series into flooding (increasing depth) and ebbing (decreasing depth) tidal phases and calculated the difference in SSC on the flood versus ebb tide over both time periods. We computed and compared 95% confidence intervals for all SSC values.

Sediment deposition on top of ceramic titles and plastic grids was measured to quantify spatial gradients in accretion rates across the marsh (see Pasternack and Bush 1998). The sediment tiles and grids were installed in June 2016 in two shore parallel transects centered on the marsh turbidity sensors (Figure 1c). Five replicates of both the sediment tiles and grids were deployed at each of these transects. The sediment tiles were drawer-liner paper (to give a rough surface) glued to the top of a 15.5cm x 15.5cm ceramic tile affixed to a PVC stake (Figure 3c). The stakes were pushed into the sediment so that the top of tile was flush with the surface. We cut 14.5cm x 14.5cm squares from fluorescent tube lighting covers which were plastic grids with 1.5cm^2 openings. The grids were then staked flush to the initial marsh surface. The openings in the grids allowed vegetation to grow through them, giving a natural surface.

The use of these sediment tiles and grids allowed for the calculation of mass accumulation rates and cumulative surface changes, respectively. All of the sediment accumulated on sediment tiles was scraped off during each subsequent visit, dried and weighed. This resulted in a mass of sediment per amount of time between visits, i.e. a mass accumulation rate. The sediment tiles were reinstalled flush with the marsh surface after each collection. The plastic grids function similarly to marker horizons. The difference between the sediment surface and grid surface was measured at each subsequent visit. A positive difference represents net deposition, while a negative difference represents net erosion. The difference between the sediment tile surface and

158 sediment surface was only measured after the surface dropped below the tile. We
159 averaged the cumulative vertical change in sediment surface height for each turbidity
160 sensor location (edge or interior) for each site visit.
161
162 Post-dieback Measurements
163 In response to the unexpected dieback event, we made a variety of other
164 measurements in spring 2017 to better quantify the dieback and its impact. All post-
165 dieback measurements were collected at three sites: the dieback area, a north
166 reference area, and a south reference area. The dieback area refers to the site where
167 initial monitoring began. The north reference area and the southern reference area are
168 both vegetated reference sites approximately 10 and 20m from the dieback area,
169 respectively (Figure 1c), where vegetation dieback did not occur. The north reference
170 site is approximately 10 m from a small creek to the north.
171 To address the changes in elevation and marsh surface profiles associated with
172 the dieback, we measured elevation along shore-normal transects using a Topcon RTK
173 GPS system. We measured elevation along two transects for each the north reference
174 area and the south reference area, totaling four “vegetated” topographic profiles. We
175 measured along three transects through the dieback area, one along the turbidity
176 sensor transect, and two intersecting the north and south ends of the sediment tile and
177 grid transects (Figure 1c). All elevations were recorded relative to NADV88. Individual
178 profiles were linearly interpolated between measured points to calculate an average
179 topographic profile for vegetated and dieback areas.

To quantify the differences in shape between the average dieback profile and the average vegetated profile, we calculated the presence/location of any inflection points. A concave up marsh topographic profile implies erosion whereas a concave down profile implies deposition (Kirby 2000, Wilson and Allison 2008, Mariotti and Fagherazzi 2010). For this we first performed a coarse smoothing spline and then calculated the second derivative. The presence and location of inflection points was defined as the location where the second derivative is equal to zero.

We calculated a loss of elevation in the dieback area by comparing the dieback topographic profile to the vegetated profile. We calculated the average difference in elevation between the vegetated profile and the portion of the dieback profile without living plants to determine a magnitude of elevation loss. From this value, we subtracted any measured erosion from the sediment tiles and plastic grids to produce an upper bound of possible subsidence. To approximate the volume of sediment lost we performed a low and high-end estimate. For the low-end estimate, we determined what volume of sediment would be required to fill the topographic concavity that was evident in the region of dead vegetation. For the high-end estimate, we assumed the topographic profiles were initially similar, and then determined the amount of sediment required to fill in the dieback profile so that it would not be statistically different than the vegetated profile

We collected sediment cores to determine if the vegetation death extended to belowground components of the plant. Specifically, we collected five cores (5cm diameter by 15cm length) from each area (i.e. the dieback area, north reference, and south reference areas). We washed each core over a 1mm sieve to extract

belowground biomass. Rhizomes were collected and classified as living or dead based on color, turgor pressure, and attachment to other living material. The total number of live and dead were pooled for each of the three locations. We conducted a z-score test for population proportions for the percent of living rhizomes to determine significance (α=0.05).

We measured in situ soil shear strength with a shear vein to determine the role the dieback may have played in affecting soil erodibility. The 50.8 x 101.6 mm head of a Humboldt H-4227 shear vein was inserted completely into the soil and was turned until the soil broke, giving a strength reading that represents the top 10 cm of the soil (after Howes et al. 2010). We performed this test with 15 replicates in the area affected by the dieback, and corresponding locations in the north reference, and south reference sites. We averaged results for each location and compared them with an ANOVA (α=0.05) to determine significance.

Results

Suspended Sediment Concentration

Measurements of SSC differ slightly from before versus after the dieback (Figure 4). The magnitude of SSC after the dieback is marginally significantly higher than before the dieback at the creek and interior locations (Figure 4a). Prior to the dieback, SSC was 41.2mg/L ± 2.45, 37.7 mg/L ± 1.00, and 22.8 mg/L ± 0.68 respectively for the creek, edge, and interior (mean and 95% confidence interval). After the dieback the SSC was 45.7 mg/L ± 1.85, 39.0 mg/L ± 1.27, and 24.7 mg/L ± 0.71 respectively for the

creek, edge, and interior. SSC decreases with distance into the marsh both pre- and post-dieback.

The difference between flood tide SSC and ebb tide SSC, or flood-ebb differential, also differs before and after the dieback. The flood-ebb differentials were all small in magnitude and positive, with most not being statistically different than zero. The flood-ebb differential was smaller after the dieback than before the dieback, but only significantly different at the marsh edge location (Figure 4b).

Deposition and Erosion.

Our seasonal measurements of sediment deposition and erosion indicate that the dieback event is contemporaneous with a switch from rapid deposition to rapid erosion at the marsh edge. For the first two months of measurement, both the marsh edge (Figure 5a) and interior sites (Figure 5b) experienced net positive changes in surface elevation measured over the plastic grids totaling 19.2mm ± 12.1 (mean ± 1σ) and 7.5mm ± 2.5 of deposition, respectively. Both sites also had positive mass accumulation measured with the sediment tiles (a maximum of 0.72g/day ± 0.41 at the edge and 0.25g/day ± 0.25 at the interior). Immediately following the dieback in December 2016, the edge site lost elevation compared to the initial elevation (-4.4mm ± 14.4) whereas the undisturbed interior site continued to gain elevation (8.7mm ± 3.1 in December 2016, totaling 24.0mm ± 6.8 by the end of May 2017). Similarly, the mass accumulation rate at the edge site quickly decreased to near zero following the dieback whereas the undisturbed interior maintained positive mass accumulation (a maximum of 0.73g/day ± 0.35 by the end of May 2017, Figure 5c-d). The change from accretion to erosion at the

edge site meant that the sediment tiles were no longer useful in measuring mass accumulation, but could be used to quantify erosion by measuring the gap between the sediment surface and the sediment tile. We found consistent patterns between the sediment tiles and plastic grids. The maximum elevation loss at the edge, as evidenced by the difference between the August surface elevation and the late-spring, is -33.5 mm ± 27.5 based off the sediment tiles and -28.5 mm ± 13 based off the plastic grids. Following a late-spring minimum, there was an increase in surface elevation at the edge, evidenced by both the sediment tiles and plastic grids.

Elevation profiles through the dieback and reference areas also reveal impacts of vegetation mortality on sediment deposition and erosion (Figure 6). The vegetated profile and the region of the dieback profile with living plants are both concave down, indicating deposition (Mariotti and Fagherazzi 2010). However, the profile through the portion of the dieback area with dead plants is concave up, consistent with an erosional profile (Kirby 2000, Wilson and Allison 2008). The average elevation difference between the vegetated profile (green) and the area of the dieback without living plants (blue dashed line) was 39.1 cm ±4.1.

To calculate an amount of sediment absent from the dieback topographic profile, we calculated low and high-end estimates. For the low-end estimate of sediment missing from the dieback profile, we drew the longest line possible within the devegetated zone such that the line was always above the profile (thin black line, Figure 6b). The difference in area between this line and a high-order polynomial approximation of the dieback curve was 0.15 m^3/meter of shoreline, which represents the minimum amount of sediment that would be required to eliminate the concave up nature of the

dieback profile. For the high-end estimate, we calculated the average amount of sediment needed to eliminate statistical differences between the dieback and vegetated profiles. We calculated the area between a high-order polynomial approximation of the average vegetated profile and one for the dieback profile. We set horizontal bounds to this area at the creek edge and at the maximum distance from the creek for which the vegetated curve was still statistically different from dieback curve. This maximum distance was approximately where the confidence bands begin to overlap, farther inland than the concave up region used to calculate the low-end estimate (Figure 6b). Assuming the dieback profile was originally similar to the vegetated profile, we calculate that 1.62 m^3/meter of shoreline of sediment is missing. If the dieback profile was initially lower than the vegetated profiles, this would represent an overestimation.

Soil Characteristics

Rhizome mortality and soil strength measurements demonstrate that the effect of the vegetation dieback included subsurface soil properties. The dieback area had a significantly lower proportion of living rhizomes (2.6%, n=39) than the north reference area (32%, n=38) and the south reference area (39%, n=23) ($p<0.001$ for both; Figure 7a). There was no significant difference in rhizome mortality between the two reference areas ($p=0.55$). Rhizomes were found in all cores, and each area had some cores without any living rhizomes. The dieback area shear strength was 1.45 kPa ± 1.18, the north reference area was 3.38 kPa ± 1.25, and the south reference area was 3.53 ± 1.17 (Figure 7b). The dieback area had significantly weaker soil than the reference

areas (ANOVA $p<0.0001$), and there was no significant difference in soil shear strength between the reference areas ($p=0.73$).

Discussion

Salt mash dieback can be caused by a number of factors including drought (Alber et al. 2008), herbivory (Holdredge et al. 2009, Smith 2009, Smith and Green 2015), salt stress (Hughes et al. 2012), soil toxicity (Mckee et al. 2004), human-induced disturbances, such as oil spills (Silliman et al. 2012, Lin et al. 2016), wrack deposits (Fischer et al. 2000), and interactions between these factors (Silliman et al., 2005). Although it is difficult to determine the initial cause of a dieback after it has occurred (Ogburn and Alber 2005), wrack deposition is a common source of dieback in the region (Li and Pennings 2016). The dieback size (e.g. 10s of meters) and creek-adjacent location, is consistent with wrack-induced diebacks elsewhere in the Altamaha estuary. (Lottig and Fox 2007). Our site was located near a drainage creek which suggests multidirectional flow, making it particularly vulnerable to wrack deposits (Li and Pennings 2016). However, we did not observe wrack during site visits meaning that any wrack deposits would have been short-lived, and perhaps insufficient to cause the dieback.

Regardless of the initial cause, the dieback affected above and belowground biomass, leading to a weakening of the soil. The site lost over 12 m^2 of marsh plants above ground and the rhizome analysis shows extensive belowground mortality (Figures 3a and 7a). The death of the rhizomes is thought to be necessary for soil

315 weakening (Silliman et al. 2012). Our results support that interpretation, where areas
316 with high rhizome mortality had a significantly lower soil shear strength (Figure 7).
317 At our site, the loss of vegetation and soil strength led to erosion and possibly
318 subsidence. Previous work in the system suggests diebacks that occur late in the
319 growing season (i.e. September, like this event) produce the greatest plant mortality and
320 loss of biomass (Li and Pennings 2017). We measured approximately 3 cm of erosion
321 based off the sediment tiles and plastic grid measurements (Figure 5a and b), whereas
322 the elevation profile of the dieback area was approximately 40 cm below the reference
323 vegetated sites (Figure 6). If we assume the dieback area and the reference areas
324 began at the same height, and the dieback experienced 3 cm of erosion, then the area
325 would have experienced a maximum of 37 cm of subsidence. However, it is possible
326 that the dieback area was initially lower than the reference areas before the death of the
327 plants. Therefore, 37 cm of subsidence represents an extreme upper bound. An initial
328 low elevation may have even contributed to the dieback location since the likelihood of
329 wrack deposition increases with decreasing marsh elevation (Bertness and Ellison
330 1987).
331 Both erosion and subsidence have been observed in other marsh dieback events
332 (Hughes et al. 2009, Baustian et al. 2012, Wilson et al. 2012). Studies of vegetation
333 death in Bayou Chitigue, LA USA, found an elevation decrease of about 8 cm during a
334 timeframe comparable to ours (DeLaune et al. 1994, Day et al. 2011). No erosion was
335 observed during the first year and all of the change in elevation was attributed to
336 subsidence caused by root decomposition and a loss of turgor pressure (DeLaune et al.
337 1994, Day et al. 2011). Monitoring for a second year discovered ~7 cm additional

338 elevation loss, 2-3 cm of which was erosion (Delaune et al. 1994). A study in Bayou
339 Lafourche, LA USA found that even with marginal surface vertical accretion of 0.2
340 cm/year, an unvegetated dieback area still lost elevation at nearly 1 cm/year (Baustian
341 et al. 2012). In a study in Cape Romain, SC USA, vegetation dieback area at the head
342 of expanding creeks were 60cm lower than the vegetated platform, caused by both
343 subsidence and erosion (Hughes et al. 2009). This severe elevation loss occurred at the
344 bottom of an incipient channel (Hughes et al. 2009) and likely represents an extreme
345 and specific example. The erosion at our site (3 cm) is therefore consistent with values
346 from similar settings presented in the literature, and the upper bound of possible
347 subsidence (37 cm) likely represents an overestimation.
348 Our results offer some limited support to the idea that sediment eroded from the
349 marsh edge becomes a source of sediment to other areas of the marsh. This marsh
350 cannibalization process, which is found in some numerical and conceptual models, has
351 been suggested to enhance overall marsh resiliency to SLR (Mariotti and Carr 2014,
352 Currin et al. 2015, Hopkinson et al. 2018). Field evidence to support this hypothesis is
353 limited. One study in Blackwater, MD USA found that marshes with high edge erosion
354 had a higher SSC and vertical accretion than stable areas (Ganju et al. 2015). In Plum
355 Island, MA USA, SSC increased further upstream eroding channels (Cavatorta et al.
356 2003), which could mean erosion increases sediment availability. Additionally, recent
357 geochemical analysis and sediment budgeting suggests marsh edge erosion is an
358 important factor in maintaining elevation relative to sea level rise in Plum Island
359 (Hopkinson et al. 2018). In our study, we found only a small increase in SSC associated
360 with vegetation dieback and erosion (Figure 4), likely because of the small spatial scale

of the dieback and relatively sparse spatial sampling. Previous work suggests dieback events intensify ebb tidal flows and lead to scour (Hughes et al. 2009). Intensified ebb transport is difficult to detect via the marsh interior sensor as it is higher in the tidal frame than the dieback or via the channel sensor as the large volume of water and sediment in the channel would dilute the signal. Nevertheless, the marsh edge sensor had a significant reduction in positive flood-ebb differential, which is consistent with net erosion (Figure 4). Marsh cannibalization is therefore plausible but remains understudied.

Conclusions

Our study adds to the large body of evidence highlighting the importance of vegetation in maintaining marsh vertical accretion and limiting lateral erosion. In our study, the marsh was rapidly accreting and prograding prior to the dieback event. In the first two months of our study, the vegetated marsh edge accreted nearly 2 cm of sediment. Above and belowground vegetation mortality led to lower soil shear strength, a switch from positive to negative elevation change, and the development of an erosional topographic profile. Our work therefore demonstrates that vegetation mortality can reverse the local elevation trajectory of an otherwise rapidly prograding marsh.

Acknowledgements

We are grateful to Ellen Herbert for discussions about sampling design and site selection, and to David Walters, Tyler Messerschmidt, and Rosemary Walker for assisting with field and lab work. We appreciate the Georgia Department of Natural

Resources for providing access to the field site and to the Georgia Coastal Estuaries LTER program for providing logistical support, especially Tim Montgomery, Dontrece Smith, and Alyssa Peterson. We thank the anonymous reviewers who helped improve this manuscript. This work was funded by NSF awards 1529245, 1654374, 1426981, and 1237733, the NSF Graduate Research Fellowship Program, and the USGS Climate and Land Use Research & Development program. This is contribution number xxxx of the Virginia Institute of Marine Science.

References

Alber, M., Swenson, E.M., Adamowicz, S.C. and Mendelssohn, I.A., 2008. Salt marsh dieback: an overview of recent events in the US. Estuarine, Coastal and Shelf Science, 80(1): 1-11.

Altieri, A.H., Bertness, M.D., Coverdale, T.C., Axelman, E.E., Herrmann, N.C. and Szathmary, P.L., 2013. Feedbacks underlie the resilience of salt marshes and rapid reversal of consumer-driven die-off. Ecology, 94(7):1647-1657.

Angelini, C. and Silliman, B.R., 2012. Patch size-dependent community recovery after massive disturbance. Ecology, 93(1): 101-110.

Baustian, J.J., Mendelssohn, I.A. and Hester, M.W., 2012. Vegetation's importance in regulating surface elevation in a coastal salt marsh facing elevated rates of sea level rise. Global Change Biology, 18(11): 3377-3382.

Bertness, M.D. and Ellison, A.M., 1987. Determinants of pattern in a New England salt marsh plant community. Ecological Monographs, 57(2): 129-147.

Cavatorta, J.R., Johnston, M., Hopkinson, C. and Valentine, V., 2003. Patterns of sedimentation in a salt marsh-dominated estuary. The Biological Bulletin, 205(2): 239-241.

Currin, C., Davis, J., Baron, L.C., Malhotra, A. and Fonseca, M., 2015. Shoreline change in the New River estuary, North Carolina: rates and consequences. Journal of Coastal Research, 31(5): 1069-1077.

D'Alpaos, A. and Marani, M., 2016. Reading the signatures of biologic–geomorphic feedbacks in salt-marsh landscapes. Advances in water resources, 93: 265-275.

Day, J.W., Kemp, G.P., Reed, D.J., Cahoon, D.R., Boumans, R.M., Suhayda, J.M. and Gambrell, R., 2011. Vegetation death and rapid loss of surface elevation in two contrasting Mississippi delta salt marshes: The role of sedimentation, autocompaction and sea-level rise. Ecological Engineering, 37(2): 229-240.

DeLaune, R.D., Nyman, J.A. and Patrick Jr, W.H., 1994. Peat collapse, ponding and wetland loss in a rapidly submerging coastal marsh. Journal of Coastal Research, 1021-1030.

Duran, O.V., Moore, L. 2013. Vegetation controls on the maximum size of coastal dunes. Proceedings of the National Academy of the Sciences. 110(43): 17217–17222

Fagherazzi, S., Marani, M. and Blum, L.K., 2004. The ecogeomorphology of tidal marshes. American Geophysical Union: Washington D.C.

Fagherazzi, S., Kirwan, M.L., Mudd, S.M., Guntenspergen, G.R., Temmerman, S., D'Alpaos, A., van de Koppel, J., Rybczyk, J.M., Reyes, E., Craft, C., Clough, J.,

2012. Numerical models of salt marsh evolution: Ecological, geomorphic, and climatic factors. Review of Geophysics 50(1): doi/10.1029/2011RG000359

Fischer, J.M., Reed-Andersen, T., Klug, J.L., Chalmers, A.G., 2000. Spatial pattern of localized disturbance along a Southeastern salt marsh tidal creek. Estuaries and Coasts 23(4): 565–571

Ganju, N.K., Schoellhamer, D.H. and Bergamaschi, B.A., 2005. Suspended sediment fluxes in a tidal wetland: Measurement, controlling factors, and error analysis. Estuaries, 28(6): 812-822.

Ganju N. K., Kirwan M. L., Dickhudt P. J., Guntenspergen G. R., Cahoon D. R., Kroeger K. D., 2015. Sediment transport-based metrics of wetland stability. Geophysical Research Letters 42(19): 7992-8000.

Hardisky, M., 1978. Marsh restoration on dredged material, Buttermilk Sound, Georgia. In Proceedings of the 5th Annual Conference of the Restoration and Creation of Wetlands, 136-151.

Holdredge, C., Bertness, M.D. and Altieri, A.H., 2009. Role of crab herbivory in die-off of New England salt marshes. Conservation Biology, 23(3): 672-679.

Hopkinson, C.S., Morris, J.T., Fagherazzi, S., Wollheim, W.M., Raymond, P.A., 2018. Lateral marsh edge erosion as a source of sediments for vertical marsh accretion. Journal of Geophysical Research: Biogeosciences 123(8): 2444-2465

Howes, N.C., FitzGerald, D.M., Hughes, Z.J., Georgiou, I.Y., Kulp, M.A., Miner, M.D., Smith, J.M. and Barras, J.A., 2010. Hurricane-induced failure of low salinity wetlands. Proceedings of the National Academy of Sciences, 107(32): 14014-14019.

Hughes, A.L.H., Wilson, A.M., Morris, J.T., 2012. Hydrologic variability in a salt marsh: Assessing the links between drought and acute marsh dieback. Estuaries, Coast, and Shelf Science. 111(1): 95-106.

Hughes, Z.J., FitzGerald, D.M., Wilson, C.A., Pennings, S.C., Więski, K. and Mahadevan, A., 2009. Rapid headward erosion of marsh creeks in response to relative sea level rise. Geophysical Research Letters, 36(3): doi:10.1029/2008GL036000

Kirby, R., 2000. Practical implications of tidal flat shape. Continental Shelf Research, 20(10-11): 1061-1077.

Kirwan, M. L., Guntenspergen, G. R., D'Alpaos, A., Morris, J. T., Mudd, S. M., Temmermen, S., 2010. Limits on the adaptability of coastal marshes to rising sea level. Geophysical Research Letters 37(23): doi 10.1029/2010GL045489

Kirwan, M. L., & Megonigal, J. P. 2013. Tidal wetland stability in the face of human impacts and sea-level rise. Nature 504(7478): 53-60.

Li, S. and Pennings, S.C., 2016. Disturbance in Georgia salt marshes: variation across space and time. Ecosphere, 7(10): dx.doi.org/10.1002/ecs2.1487

Li, S. and Pennings, S.C., 2017. Timing of disturbance affects biomass and flowering of a saltmarsh plant and attack by stem-boring herbivores. Ecosphere, 8(2): 01675. 10.1002/ecs2.1675

Lin, Q., Mendelssohn, I.A., Graham, S.A., Hou, A., Fleeger, J.W. and Deis, D.R., 2016. Response of salt marshes to oiling from the Deepwater Horizon spill: Implications for plant growth, soil surface-erosion, and shoreline stability. Science of the Total Environment, 557: 369-377.

Lindstedt, D.M., Swenson, E.M., Reed, D., Twilley, R. and Mendelssohn, I.A., 2006. The case of the dying marsh grass. Report submitted to the Louisiana Department of Natural Resources, Baton Rouge, LA.

Lottig, N.R. and Fox, J.M., 2007. A potential mechanism for disturbance-mediated channel migration in a southeastern United States salt marsh. Geomorphology, 86(3-4): 525-528.

Mariotti G., Carr J., 2014. Dual role of salt marsh retreat: Long term loss and short-term resilience. Water Resources Research 50(4): 2963-2974.

Mariotti G., Fagherazzi S. 2010. A numerical model for the coupled long-term evolution of salt marshes and tidal flats. Journal of Geophysical Research 115(F1): doi:10.1029/2009JF001326

McKee, K.L., Mendelssohn, I.A. and D Materne, M., 2004. Acute salt marsh dieback in the Mississippi River deltaic plain: a drought-induced phenomenon? Global Ecology and Biogeography, 13(1): 65-73.

Morris J. T., Sundareshwar P. V., Nietch C. T., Kjerfve B., Cahoon D. R. 2002. Responses of coastal wetlands to rising sea level. Ecology 83(10): 2869-2877.

Murray, A.B., Knaapen, M.A.F., Tal, M. and Kirwan, M.L., 2008. Biomorphodynamics: Physical-biological feedbacks that shape landscapes. Water Resources Research, 44(11): doi/10.1029/2007WR006410

Ogburn, M.B. and Alber, M., 2006. An investigation of salt marsh dieback in Georgia using field transplants. Estuaries and Coasts, 29(1): 54-62.

Pasternack, G.B. and Brush, G.S., 1998. Sedimentation cycles in a river-mouth tidal freshwater marsh. Estuaries, 21(3): 407-415.

Pawlik, L., Phillips, J.D., Šamonil, P., 2012. Roots, rock, and regolith: Biomechanical and biochemical weathering by trees and its impact on hillslopes—A critical literature review. Earth-Sciences Reviews 159: 142-159.

Redfield, A.C., 1972. Development of a New England salt marsh. Ecological monographs, 42(2): 201-237.

Reed, D.J., 1995. The response of coastal marshes to sea-level rise: Survival or submergence? Earth Surface Processes and Landforms, 20(1): 39-48.

Reinhardt, L., Jerolmack, D., Cardinale, B.J., Vanacker, V. and Wright, J., 2010. Dynamic interactions of life and its landscape: feedbacks at the interface of geomorphology and ecology. Earth Surface Processes and Landforms, 35(1): 78-101.

Saco, P.M., Willgoose, G.R. and Hancock, G.R., 2007. Eco-geomorphology of banded vegetation patterns in arid and semi-arid regions. Hydrology and Earth System Sciences Discussions, 11(6): 1717-1730.

Silliman, B. R., van de Koppel, J., Bertness, M. D., Stanton, L. E., & Mendelssohn, I. A. 2005. Drought, snails, and large-scale die-off of southern US salt marshes. Science, 310(5755): 1803-1806.

Silliman, B.R., van de Koppel, J., McCoy, M.W., Diller, J., Kasozi, G.N., Earl, K., Adams, P.N. and Zimmerman, A.R., 2012. Degradation and resilience in Louisiana salt marshes after the BP–Deepwater Horizon oil spill. Proceedings of the National Academy of Sciences, 109(28): 11234-11239.

517 Smith, S.M., 2009. Multi-decadal changes in salt marshes of Cape Cod, MA:
518 photographic analyses of vegetation loss, species shifts, and geomorphic
519 change. Northeastern Naturalist, 16(2), pp.183-208.
520 Smith, S.M. and Green, C.W., 2015. Sediment suspension and elevation loss triggered
521 by Atlantic mud fiddler crab (Uca pugnax) bioturbation in salt marsh dieback
522 areas of southern New England. Journal of Coastal Research, 31(1): 88-94.
523 Steiger, J., Tabacchi, E., Dufour, S., Corenblit, D. and Peiry, J.L., 2005.
524 Hydrogeomorphic processes affecting riparian habitat within alluvial channel–
525 floodplain river systems: a review for the temperate zone. River Research and
526 Applications, 21(7): 719-737.
527 Temmerman, S., Govers, G., Wartel, S. and Meire, P., 2003. Spatial and temporal
528 factors controlling short-term sedimentation in a salt and freshwater tidal marsh,
529 Scheldt estuary, Belgium, SW Netherlands. Earth Surface Processes and
530 Landforms, 28(7): 739-755.
531 Temmerman S., Bouma T. J., Govers G., Wang Z. B., De Vries M. B., Herman P. M. J.
532 2005. Impact of vegetation on flow routing and sedimentation patterns: Three-
533 dimensional modeling for a tidal marsh. Journal of Geophysical Research
534 110(F4): doi: 10.1029/2005JF000301
535 Temmerman, S., Moonen, P., Schoelynck, J., Govers, G. and Bouma, T.J., 2012.
536 Impact of vegetation die-off on spatial flow patterns over a tidal
537 marsh. Geophysical Research Letters, 39(3): doi/10.1029/2011GL050502
538 van Belzen, J., van de Koppel, J., Kirwan, M.L., van der Wal, D., Herman, P.M., Dakos,
539 V., Kéfi, S., Scheffer, M., Guntenspergen, G.R. and Bouma, T.J., 2017.

Vegetation recovery in tidal marshes reveals critical slowing down under increased inundation. Nature communications, 8, p.ncomms15811.

Wang, C. and Temmerman, S., 2013. Does biogeomorphic feedback lead to abrupt shifts between alternative landscape states?: An empirical study on intertidal flats and marshes. Journal of Geophysical Research: Earth Surface, 118(1): 229-240.

Wieski, K, H. Guo, C.B. Craft, S.C. Pennings 2010. Ecosystem functions of tidal fresh, brackish, and salt marshes on the Georgia Coast. Estuaries and Coasts 33(1):161-169.

Wilson, C.A. and Allison, M.A., 2008. An equilibrium profile model for retreating marsh shorelines in southeast Louisiana. Estuarine, Coastal and Shelf Science, 80(4): 483-494.

Wilson, C.A., Hughes, Z.J., FitzGerald, D.M., 2012. The effects of crab bioturbation on Mid-Atlantic saltmarsh tidal creek extension: Geotechnical and geochemical changes. Estuarine, Coastal and Shelf Science, 106:33-44

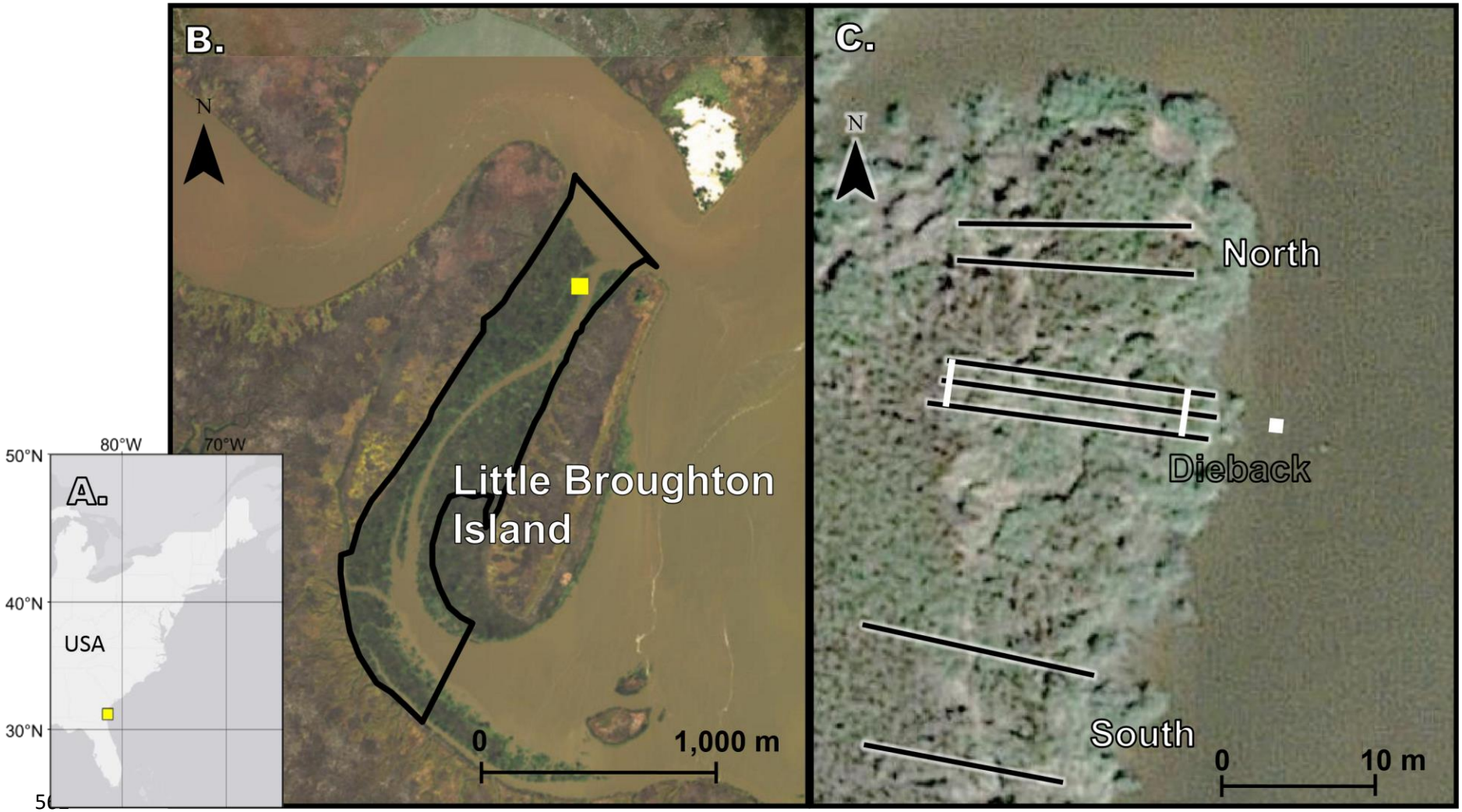

Figure 1: A. Map of U.S. east coast with study site shown in yellow square. B. Regional scale site map, with a thick black line that outlines the area of open water in 1975. For all subsequent years, the 1975 polygon is used as a boundary and open water area within it is calculated. The yellow square marks the specific study site, detailed in C. Shore-normal black lines indicate topographic profiles and shore-parallel white lines indicate sediment tile

568 and grid transects. The middle black line in the dieback zone is the sensor transect. The creek sensor is located at the white square, the marsh
569 sensors are located at the intersections of the sediment tile and grid transects and the sensor transect

570

571

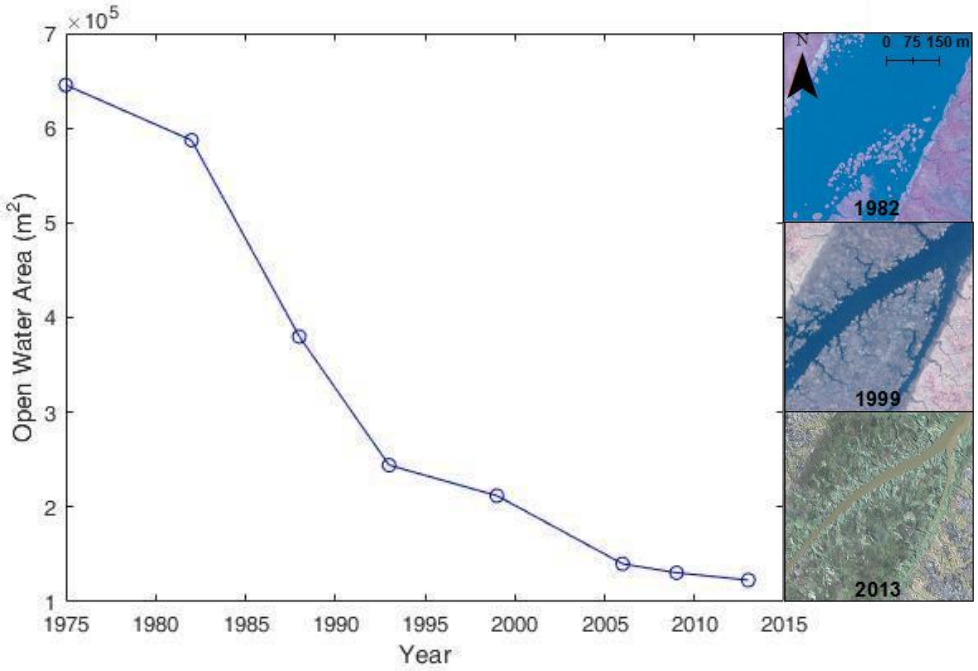

Figure 2: Area of open water within the study area (Figure 1b) was inferred from aerial photography from 1975 to 2013. Sample photos from 1982, 1999, and 2013 demonstrate the decrease in open water is attributable to lateral marsh expansion.

572
573

574

Figure 3: A. The site at maximum dieback extent in March 2017. Short, dead plant stems mark the former extent of tall, living vegetation at beginning of the study. B. Exposed rhizomes of *Spartina alterniflora* from late-spring 2017. C. Undercut sediment tile and exposed *S. alterniflora* roots from late-spring 2017.

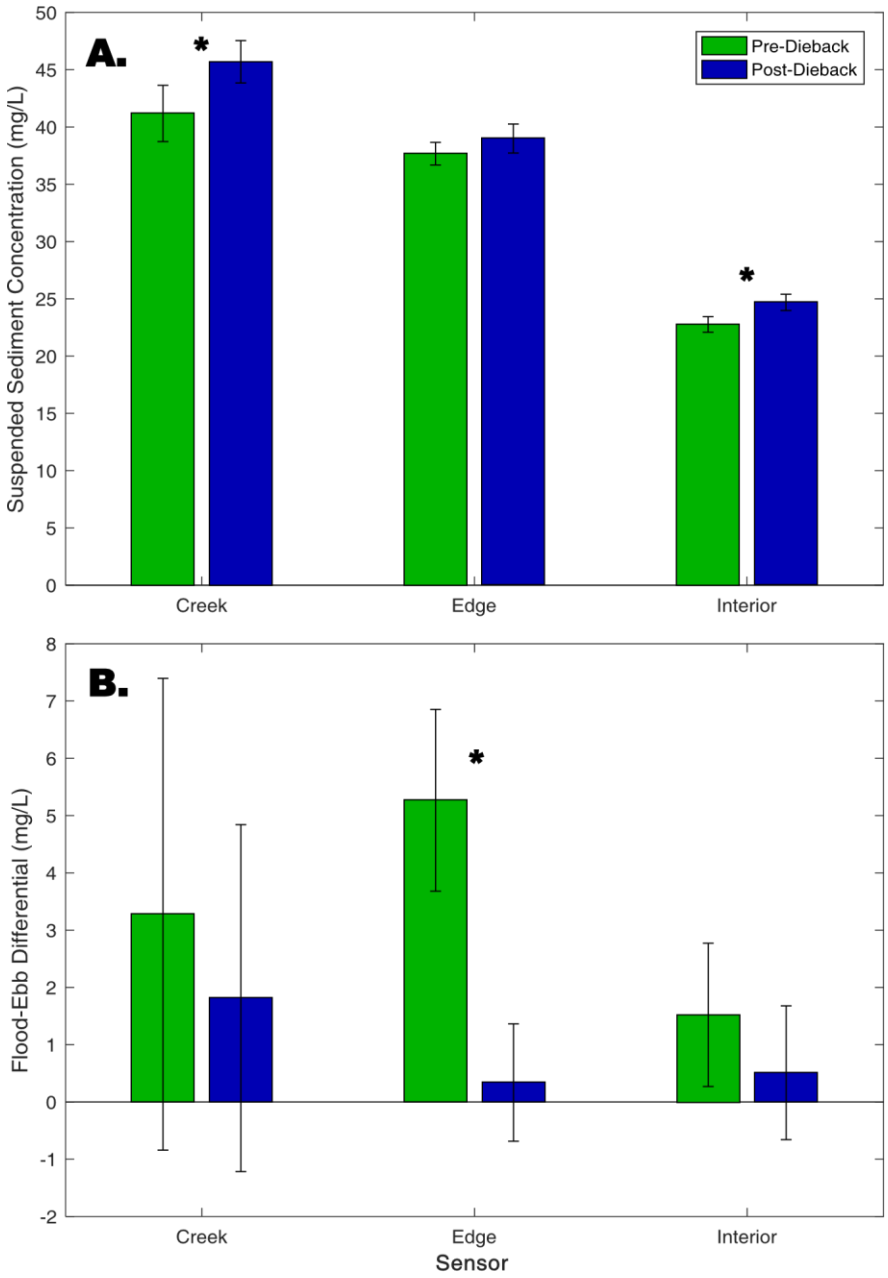

Figure 4: A. Average suspended sediment concentration of the flooded marsh before (green) and after (blue) the dieback. B. Flood-ebb differential before (green) and after (blue) the dieback, with positive values indicating higher SSC on the flood tide. Asterisks indicate locations in which the 95% confidence interval (black error bars) from before the dieback does not overlap with the interval from after the dieback.

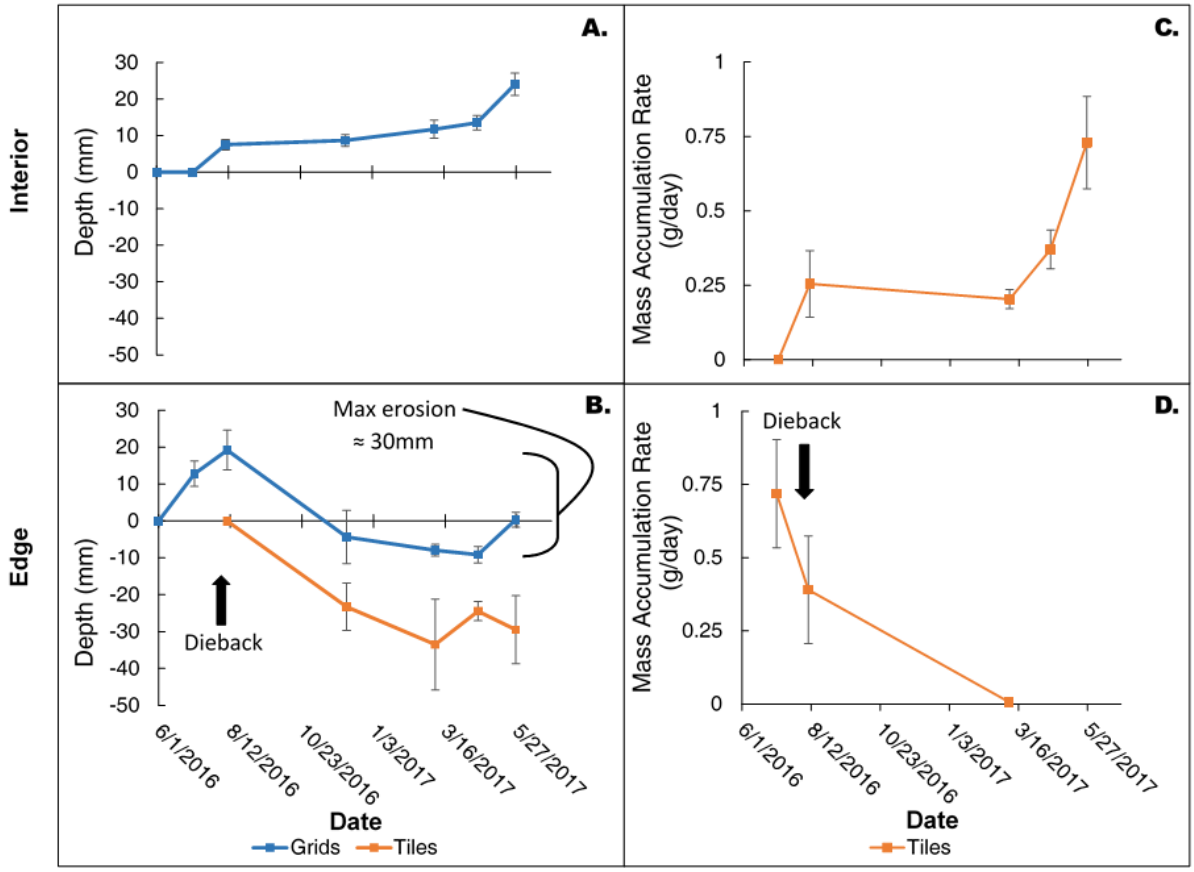

Figure 5: A. and B. Cumulative measures of elevation change, with initial values of zero and increasing values indicating accretion on the plastic grid (blue) or sediment tiles (orange). Decreasing values indicate erosion. C. and D. Mass accumulation rate of sediment on top of the sediment plates calculated per days since last collection. Top panels are the interior while the bottom panels are the edge which directly experienced the dieback. Error bars represent standard error of the mean. The approximate time of the dieback is indicated. Tiles at the edge (B. and D.) were used to measure mass accumulation until the dieback, when they were then used to measure sediment depth.

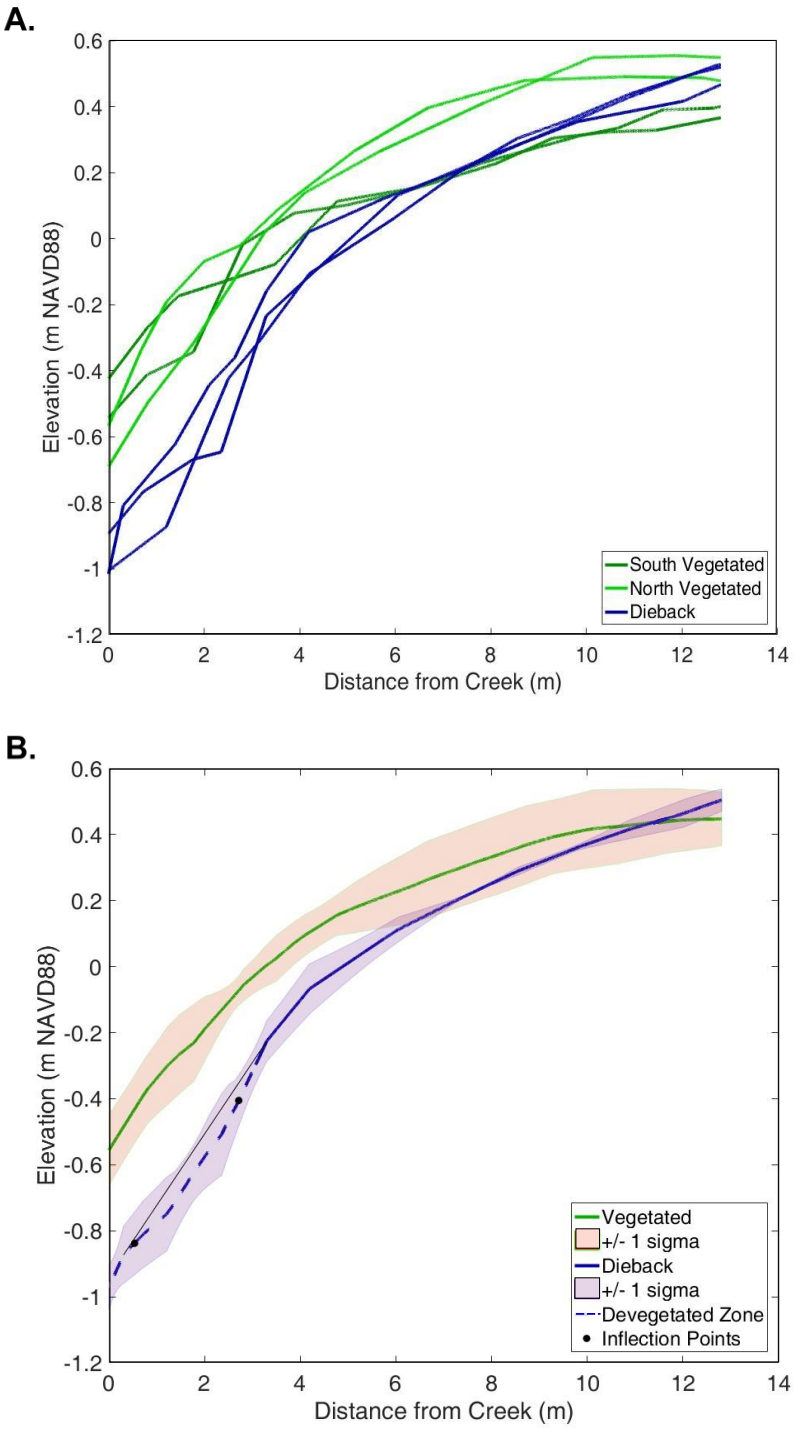

Figure 6: A. Individual elevation profiles for the South Reference (dark green), North Reference (light green) and Dieback (blue) sites. B. Average elevation profiles (± 1 standard deviation) for the vegetated (green line) and dieback areas (blue line). Black points represent inflection points used to quantify differences in curve shape. The dashed component of the dieback line indicates area without vegetation. The line used for the low-end sediment volume loss calculation is represented by the thin black line.

605

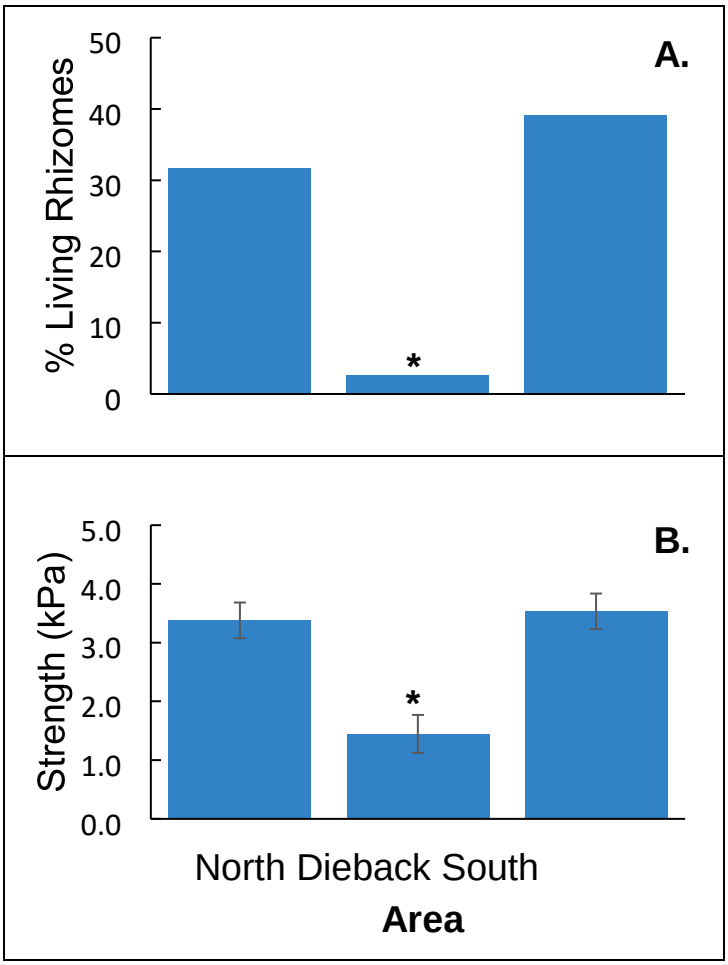

606 Figure 7: A. Pooled percentage of living rhizomes for each area. B. Average soil shear strength for each
607 area. The error bars represent standard error of the mean and the asterisks indicate significantly lower
608 values.

609

610